Japan Architectural Review
Open Access
Architectural Institute of Japan

Translated paper

Motion analysis of furniture under seismic excitation using the finite element method

Daigoro Isobe,[1] Takuzo Yamashita,[2] Hiroyuki Tagawa,[3] Mika Kaneko,[4] Toru Takahashi[5] and Shojiro Motoyui[6]

[1]Division of Engineering Mechanics and Energy, University of Tsukuba, Ibaraki, Japan; [2]E-Defense, National Research Institute for Earth Science and Disaster Resilience, Hyogo, Japan; [3]Department of Architecture, Mukogawa Women's University, Hyogo, Japan; [4]Corporate Planning Division, Shimizu Corporation, Tokyo, Japan; [5]Department of Architecture, Chiba University, Chiba, Japan; [6]Department of Architecture and Building Engineering, Tokyo Institute of Technology, Kanagawa, Japan

Correspondence
Daigoro Isobe, Division of Engineering Mechanics and Energy, University of Tsukuba, Ibaraki, Japan.
Email: isobe@kz.tsukuba.ac.jp

Funding information
No funding information is provided.

The Japanese version of this paper was published in Volume 80 Number 718, pages 1891-1900, https://doi.org/10.3130/aijs.80.1891 of *Journal of Structural and Construction Engineering (Transactions of AIJ)*. The authors have obtained permission for secondary publication of the English version in another journal from the Editor of *Journal of Structural and Construction Engineering (Transactions of AIJ)*. This paper is based on the translation of the Japanese version with some slight modifications.

Received July 10, 2017; Accepted September 16, 2017

doi: 10.1002/2475-8876.1015

Abstract

Improperly secured furniture, especially on the upper floors of high-rise buildings under long-period ground motion, can prove dangerous to human life. Fallen items of furniture such as chairs and desks could become fatal obstacles that prevent efficient evacuation. In this research, an effective numerical code for analyzing the motion of furniture subjected to seismic excitations was developed. The numerical code is based on the adaptively shifted integration — Gauss technique, which is a finite element scheme that provides higher computational efficiency than the conventional code. The frictional contact between objects was fully considered by employing a sophisticated penalty method. Various excitation tests of furniture were conducted on a shake-table. In the experiments, steel cabinets were excited by seismic waves and displacement data were recorded by a motion capture system. The numerical results were validated through a comparison with the shake-table test results.

Keywords
ASI–Gauss technique, finite element method, furniture, motion analysis, penalty method

1. Introduction

In the Great Hanshin-Awaji Earthquake of 1995, many injuries to people inside buildings resulted from the loss of evacuation paths caused by the tumbling and scattering of furniture, although the buildings themselves suffered no severe damage.[1] This tumbling of furniture caused nearly 50% of the injuries sustained indoors. Direct harm to humans, particularly in high-rise buildings, is to be expected if an earthquake with long-period ground motion occurs. Therefore, there is a strong need to understand the motion behavior of furniture under seismic excitations to reduce the number of indoor victims. Under these circumstances, E-Defense of the National Research Institute for Earth Science and Disaster Resilience (NIED) has been verifying the motion and damage of non-structural components such as furniture, outer walls, ceilings, and glass windows using a real-scale specimen of the top floors of a super high-rise building on a three-dimensional (3-D) shake-table (Figure 1).[2] However, as the tests should be repeatedly conducted to obtain quantitative and reliable data, the cost and time required would become enormous, and there are, of course, limitations from a financial point of view. To compensate this demerit and clarify the motions of non-structural components without being affected by such conditions as test scales and the number of tests, it is important to develop a highly sophisticated numerical code that can simulate these phenomena.

In general, numerical methods such as the distinct element method (DEM)[3] are applied to the motion analysis of furniture[4-6] and most of the outstanding works were carried out in Japan. However, it is difficult to verify the deformation and transition of stresses in the contact phase between furniture and walls, glass, or human bodies, because items of furniture are modeled as rigid bodies in the DEM. The main purpose of this study is to develop a finite element code to simulate the seismic motion behavior of furniture; this is one of the projects of the Research & Development Committee of E-Simulator,[7] conducted by the E-Defense. The numerical code was developed based upon the adaptively shifted integration (ASI)–Gauss technique,[8] which requires minimal computational cost in the structural analysis of large-scale framed structures. The frictional contact between objects was fully considered by employing a sophisticated penalty method.[9] The criteria for fixing physical parameters such as penalty coefficients and dynamic friction coefficients were clarified

Figure 1. Scattered furniture during experiments conducted by E-Defense[2]

in the process, and the numerical code was validated by comparison with various experimental results for furniture on a shake-table. Furthermore, the merits of using the finite element method (FEM) were confirmed by observing the sectional forces acting on the furniture. In this study, some seismic waves with comparatively short predominant periods, which are expected to cause complex motion behavior in furniture, were selected as input waves to verify the validity of the numerical code.

This paper is organized as follows. Section 2 introduces the numerical code and Section 3 describes the general outline of the shake-table tests. Section 4 describes the numerical models and conditions, and Section 5 presents the numerical results, which are validated using the experimental results. Section 6 concludes this paper.

2. Numerical methods

2.1 ASI–Gauss technique

The ASI–Gauss technique is a modified version of the ASI technique[10] that significantly reduces the computational cost by adaptively shifting the numerical integration points in linear Timoshenko beam elements according to their material behavior. In the ASI–Gauss technique, two consecutive elements forming a member are considered as a subset, and the numerical integration points of an elastically deformed member are placed such that the stress evaluation points coincide with the Gaussian integration points of the two-element member. In this way, the technique takes advantage of two-point integration while using one-point integration per element in the actual calculations, and the accuracy in elastic solutions can be drastically improved. Contact and slip motions between elements are simulated by implementing a contact algorithm based on a sophisticated penalty method in the numerical code using the ASI–Gauss technique.

2.2 Contact algorithm based on a sophisticated penalty method

To simulate various contact phenomena between furniture and walls or floors during seismic excitation, frictional contact between objects was considered using a sophisticated penalty method. Figure 2 shows the subjected forces and the geometrical relations between two elements, with member widths of L_1 and L_2, as they approach each other with relative velocity $\mathbf{v}$. Once the current distance l between the central lines of the two elements becomes shorter than the mean value L of the member widths of the elements, the penalty force vector $\mathbf{F_P}$, expressed as follows, is assumed to act in the normal direction of the contact plane:

$$\mathbf{F_p} = \alpha\left(1 - \frac{l}{L}\right)^q \frac{\mathbf{n}}{||\mathbf{n}||}, if(l \le L) \tag{1}$$

where α is the penalty coefficient, q is the penalty index, and $\mathbf{n}$ is the normal vector at the contact surface. The penalty force

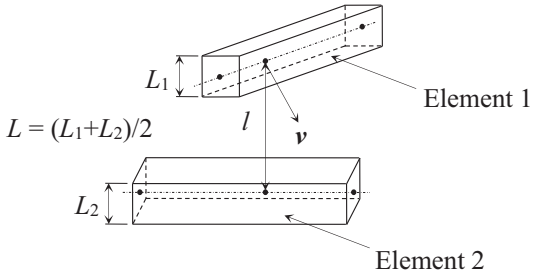

A Geometrical relations between elements

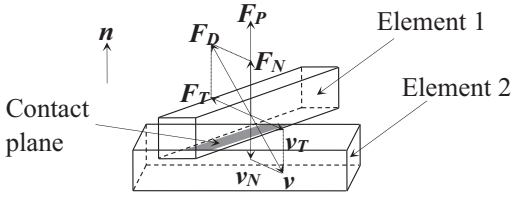

B Indent phase of elements

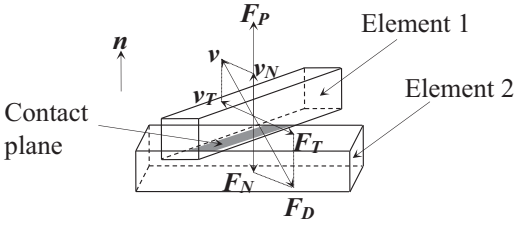

C Release phase of elements

Figure 2. Penalty force and dynamic friction force acting between elements. (A) Geometrical relations between elements. (B) Indent phase of elements. (C) Release phase of elements

vector has a constant direction regardless of the indent phase (Figure 2b) or the release phase (Figure 2c). Then, the frictional force vector $\mathbf{F_D}$ is assumed to act not only in the tangential direction of the contact plane, but also in the normal direction:

$$\mathbf{F_D} = \mathbf{F_T} + \mathbf{F_N}, if(l \le L) \tag{2}$$

where $\mathbf{F_T}$ and $\mathbf{F_N}$ are the tangential and normal components of $\mathbf{F_D}$, respectively. The vectors $\mathbf{F_T}$ and $\mathbf{F_N}$ act in the opposite directions of each component of the relative velocity $\mathbf{v}$ as follows:

$$\mathbf{F_T} = -\mu\alpha\left(1-\frac{l}{L}\right)^q \frac{\mathbf{v_T}}{||\mathbf{v_T}||}, if(l \le L) \quad (3)$$

$$\mathbf{F_N} = -D_C\left(1-\frac{l}{L}\right)^q \frac{\mathbf{v_N}}{||\mathbf{v_N}||}, if(l \le L) \quad (4)$$

where μ is the dynamic friction coefficient, D_c is the damping coefficient in the normal direction, $\mathbf{v_T}$ is the tangent component of $\mathbf{v}$, and $\mathbf{v_N}$ is the normal component of $\mathbf{v}$. The component in the normal direction $\mathbf{F_N}$ acts in different directions depending on the phases (indent or release), and the magnitude varies according to the sizes of the contact depth and relative velocity; this component acts as a damping force along the contact depth and contributes to maintain numerical stability. The parameters shown above are fixed according to simple rules, explained later in this paper, by referring to the masses of objects and the static friction coefficients of the floors and walls.

3. Outline of shake-table tests

In this study, tests were performed using a hydraulic 3-D shake-table belonging to Shimizu Corporation. The table has plane dimensions of 4 m × 4 m, and the tests proceeded by varying the seismic waves, input levels, and the number of excitation directions. Various items of furniture were arranged on the shake-table, mimicking an office room. Two walls made of plywood nailed to a light-steel base and steel frames faced each other, and a set of furniture was positioned on a floor covered by a carpet. A motion capture system (VENUS3D-250N; Nobby Tech. Ltd., Tokyo, Japan) was used to take 3-D measurements of the motion of the furniture and floor. The system was introduced to improve the reproducibility of the numerical code by conducting a detailed validation with 3-D displacement data of furniture, including the overturning phase. The camera has 0.69 million pixels with a sampling frequency of 250 Hz. The system measures multiple points at the same time without contact, and analyzes 3-D displacements and velocities. Furthermore, it brings out only the motions of furniture by computing the differences in motion of the entire measured space using a relative coordinate calculation function. As shown in Figure 3, the locations of luminous markers attached to the furniture and the floor were measured by a total of six infrared cameras, three from both sides.

An overview of the five types of furniture used as specimens is shown in Figure 4. The cross-section shapes of members used in the furniture were all hollow structures with a thickness of 2 mm. The three types of cross-sections shown in Figure 5 were used. The cross-section parameters for each item of furniture are presented in Table 1, and the sizes and physical parameters are shown in Figure 6 and Table 2, respectively. The static friction coefficients measured beforehand between each item of furniture and the carpet floor on the shake-table are also given in Table 2, along with the sizes, weights, and location of center of gravity. The static friction coefficients were evaluated by pulling the base of the furniture with a spring scale, and by dividing the mean value of the force required to move the furniture (averaged over three tests) by the weight of the furniture. The static friction coefficient of the upper, separated cabinet was measured on the top board of the lower cabinet.

Experiments were performed on the following three configurations of furniture by setting the two walls orthogonal to the excited direction under one-dimensional (1-D) excitation. Each configuration of furniture at the initial state is shown in Figure 7.

1. Configuration 1: tall cabinet and separated cabinets placed beside one of the walls.
2. Configuration 2: side table, desk, and office chair placed back from the walls. Clearances were maintained to prevent interference as furniture fell down.
3. Configuration 3: tall cabinet and separated cabinets placed beside one of the walls; side table, desk, and office chair placed near to the center.

The data obtained from configurations 1 and 2 were used to set the physical parameters of each item of furniture, because there was less interference between the furniture in these configurations.

The JMA-Kobe wave observed during the 1995 Great Hanshin-Awaji Earthquake, as shown in Figure 8, and the KiK-net Haga wave observed during the 2011 Great East-Japan Earthquake, as shown in Figure 9, were used as the input waves. The excitation program is listed in Table 3. Both 1-D and 3-D excitations at 50% and 100% of the original waves were applied in each configuration. The north–south (NS) component of the JMA-Kobe seismic wave and the east–west (EW) component of the KiK-net Haga seismic wave were applied in the *X*-axis direction; only the *X*-axis direction was excited in the case of 1-D excitation.

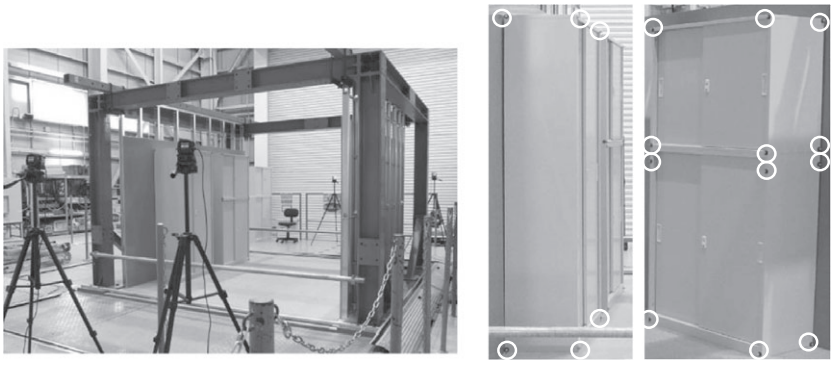

A Cameras around the shake-table **B** Locations of the markers

Figure 3. Motion capture system and the configurations of markers. (A) Cameras around the shake-table. (B) Locations of the markers

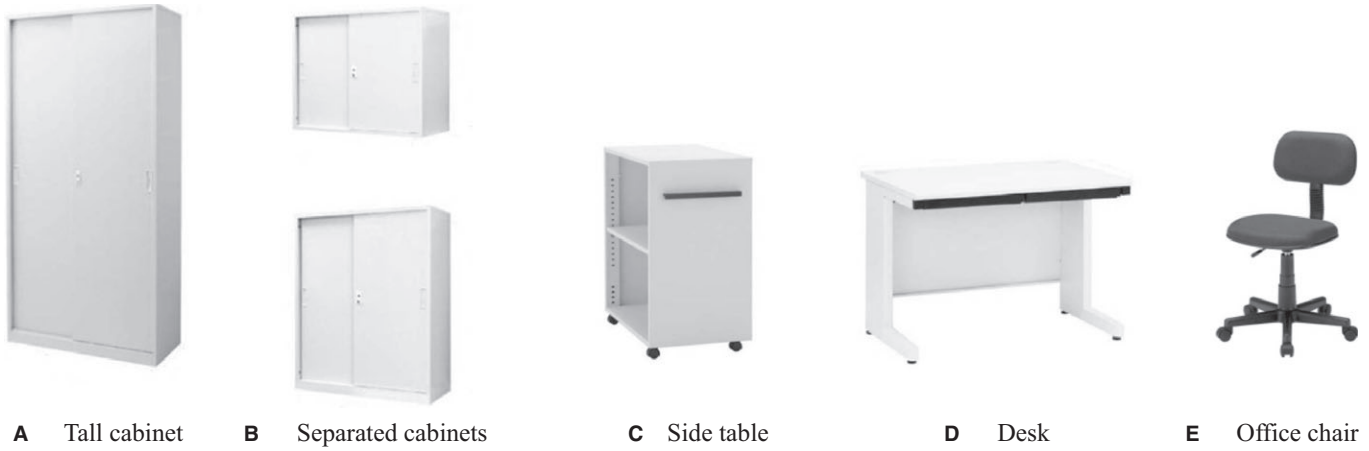

Figure 4. Set of furniture placed on the shake-table. (A) Tall cabinet. (B) Separated cabinets. (C) Side table. (D) Desk. (E) Office chair

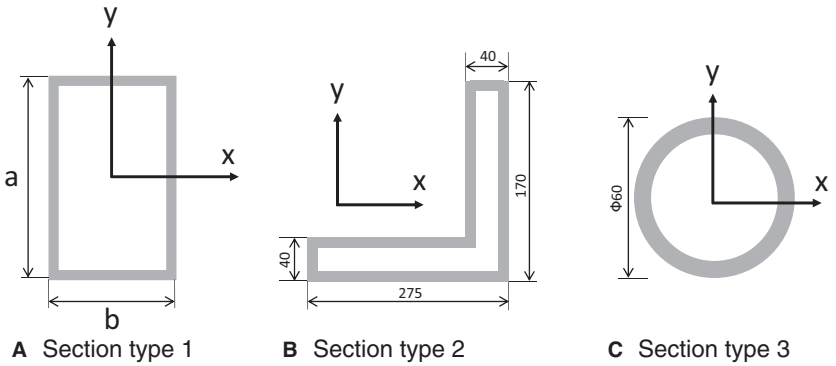

Figure 5. Cross-section types of members (unit: mm). (A) Section type 1. (B) Section type 2. (C) Section type 3

Table 1. Cross-section parameters of furniture used in shake-table tests

Member in furniture	Section type	a (mm)	b (mm)	Sectional area (mm^2)	Moment of inertia around x-axis (mm^4)	Moment of inertia around y-axis (mm^4)
All members of cabinets and desk	Type 1	50	30	304	1.016×10^5	4.513×10^4
Front columns of side table	Type 1	170	40	824	2.654×10^6	2.613×10^5
Rear columns of side table	Type 2			1764	1.488×10^7	4.867×10^6
Beams of side table	Type 1	445	40	1924	3.644×10^7	6.587×10^5
Backrest of office chair	Type 1	300	80	1504	1.575×10^7	1.972×10^6
Seat surface of office chair	Type 1	400	80	1904	3.337×10^7	2.580×10^6
Base of office chair	Type 3			704	2.773×10^5	2.773×10^5

4. Numerical models and conditions

Linear Timoshenko beam elements were used to model the furniture under the ASI–Gauss code. As mentioned, the cross-section types shown in Figure 5 were used for each item of furniture. More elements were used in furniture items that were expected to make frequent contact, because a coarse element subdivision might underestimate the contact between furniture and allow items to pass through each other. In this study, larger numbers of elements were introduced to the tall cabinet, separate cabinets, and desk. The subdivided element length was fixed to 50 mm, the same value as the member width of the furniture. To reduce the computational cost, the floor and walls of the shake-table were not modeled by finite elements; the penalty forces and frictional forces applied by the furniture in the contact phase were neglected, and it was assumed that the floor and walls were not deformed during the process. The contact between the floor/walls and the furniture was numerically determined using the differences of the nodal coordinates. The center of gravity for each item of furniture (see Table 2) was considered by adjusting the member densities. The furniture items made of steel had the following material properties: Young's modulus 206 GPa, Poisson's ratio 0.3, and yield stress 245 MPa. The constructed numerical models are shown on the right in Figure 7. In both the experiments and the analyses, the set of furniture was placed according to the drawing on the left. The total numbers of elements for each model were 5056, 1005, and 6041, and the total numbers of nodes were 3804, 788, and 4574 for configurations 1, 2, and 3, respectively.

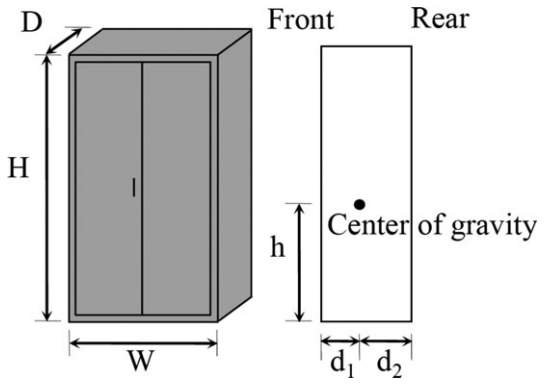

Figure 6. Sizes of furniture

The acceleration data measured on the shake-table under the JMA-Kobe wave and the KiK-net Haga wave were used as the input waves for the numerical analyses. The data obtained from the markers on the shake-table when the JMA-Kobe wave was applied, along with the acceleration response spectrum, are shown in Figures 10 and 11, respectively. Similarly, the data and the acceleration response spectrum obtained when the KiK-net Haga wave was applied are shown in Figures 12 and 13, respectively. These data were obtained by differentiating the displacements obtained by the motion capture system twice and by cutting off 10 Hz and higher frequencies. The predominant periods of the former waves were 0.47 s (NS) and 0.73 s (EW), and those of the latter waves were 0.60 s (NS) and 0.43 s (EW).

Contact parameters such as the penalty coefficients used in the analyses were configured as follows. The penalty coefficients α were assumed to become larger or smaller depending on the weight of the furniture, and the weight values were directly adopted as the coefficients. A penalty index q controls the relation between indentation depth and contact force applied between objects; this relation was assumed to be linear, and the index value was uniformly set to 1. The dynamic friction coefficients μ between the furniture and the floor were evaluated based on the data observed in configurations 1 and 2 (see Figure 7), and were fixed to 80% of the static friction coefficients measured beforehand on the shake-table. As the static friction coefficients between the furniture and walls were not available, their μ values were assumed to be the same as those along the longer edge direction of the furniture on the floor. The μ values between items of furniture were fixed to 80% of the static friction coefficient measured between the separated cabinets. The damping coefficient D_c prevents excessive rebound or indentation between elements. If D_c is too small, intense vibrations are caused by the trade-off between the penalty force applied from the floor and the furniture weight. However, if D_c is too large, the rocking motion of the furniture may be damped. The D_c values were evaluated based on the data observed in configurations 1 and 2, and were fixed to 120% of the penalty coefficients. The contact parameters of the furniture used in the analyses are listed in Table 4. These values were used throughout the analyses in the same manner.

The conjugate gradient method was used for the solver, and the updated Lagrangian formulation was used for the nonlinear incremental theory. Newmark's β method with numerical damping ($\beta = 4/9$) was used for the time integration scheme, and the time increment was set to 1 ms. The total computational times were about 16 h for configuration 1, 1.5 h for configuration 2, and 30 h for configuration 3 using a standard personal computer with an Intel Core i7 3.5 GHz processor and 16 GB RAM.

5. Validation of the numerical results with experimental results

The motion of the furniture should change depending on the input wave, friction coefficient of the contact face, and furniture configuration. A single item of furniture would make rocking or translational motions and eventually tumble. Overlaid furniture such as separated cabinets would exhibit very complex behavior; the whole cabinet could fall in one piece, or the upper cabinet may tumble after making rocking and translational motions on the lower cabinet. Furniture with casters would generally slide along the floor. There was much less contact between furniture in configurations 1 and 2 (see Figure 7), and the qualitative motion of furniture described above was observed. More complex behavior such as contact between furniture and sliding motion was observed in configuration 3, involving all five items of furniture. Therefore, this paper compares the experimental and numerical results for this configuration. The appearance of the furniture at the final state of experiments and analyses for the input cases of (i) 50% JMA-Kobe wave, 1-D excitation, (ii) 100% JMA-Kobe wave, 1-D excitation, (iii) 100% JMA-Kobe wave, 3-D excitation, and (iv) 100% KiK-net Haga wave, 3-D excitation, are shown in

Table 2. Physical parameters of furniture used in shake-table tests

Symbol	Types of furniture	Size (mm)	Weight (kg)	Location of center of gravity (mm)			Material	Coefficient of static friction	
				h	d_1	d_2		Longer edge direction	Shorter edge direction
①	Tall cabinet	W900 × D400 × H1850	43.6	925	178	222	Steel	0.348	0.260
② upper	Upper, separated cabinet	W900 × D400 × H730	21.3	365.5	171	229	Steel	0.211[a]	0.211[a]
② lower	Lower, separated cabinet	W900 × D400 × H1120	28.8	562	179	221	Steel	0.336	0.289
③	Side table	W550 × D340 × H617	8.0	308	218	122	Steel	0.180	0.117
④	Desk	W1200 × D700 × H700	30.5	600	380	320	Steel	0.471	0.443
⑤	Office chair	W520 × D520 × H810	6.2	423	260	260	Steel and plastic	0.081	0.048

[a]Measured on the top board of the lower cabinet. Other items of furniture were measured on the carpet floor.

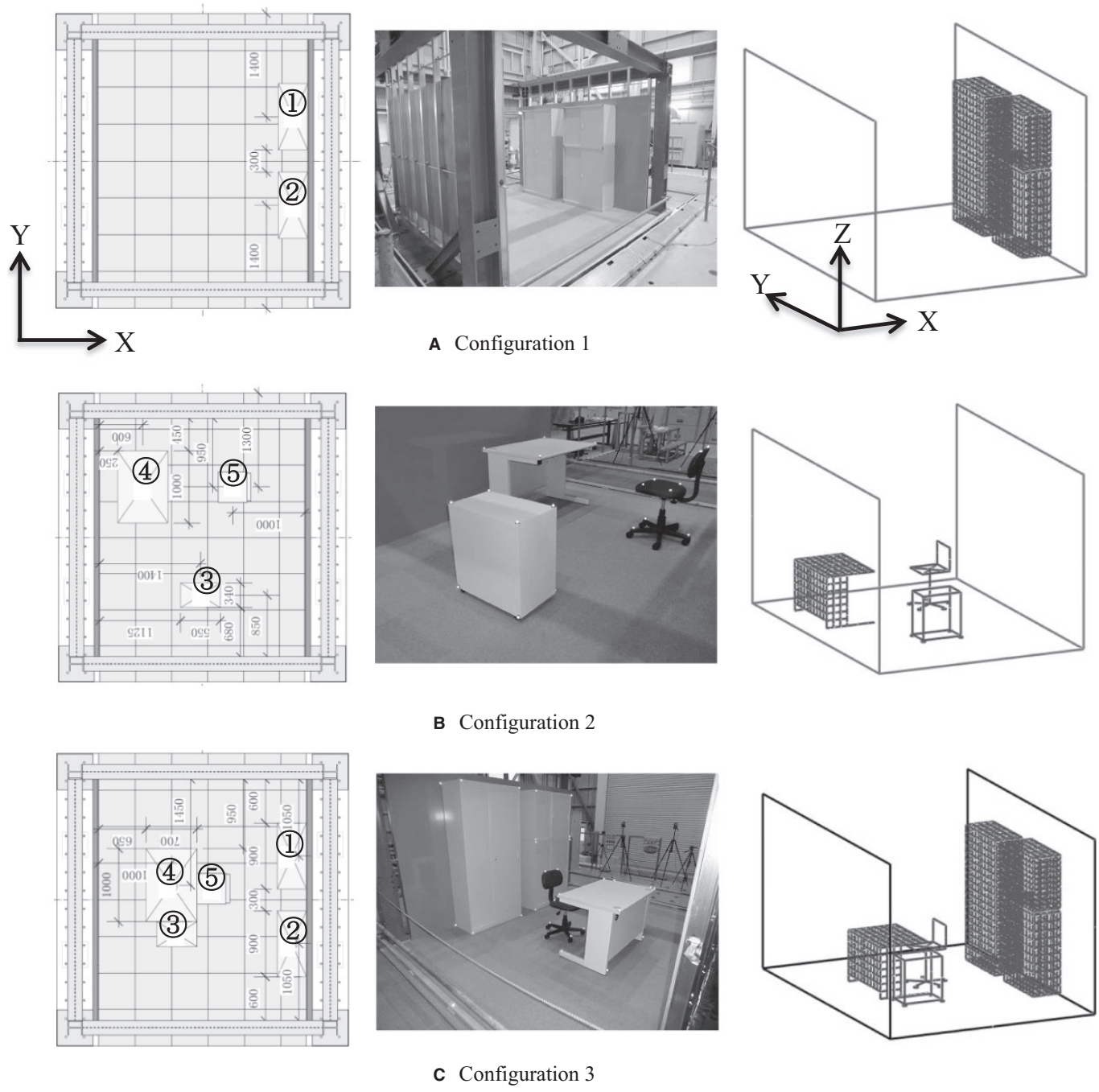

Figure 7. Configurations on the shake-table (From left: drawing, appearance on the shake-table and numerical models, unit: mm). (A) Configuration 1. (B) Configuration 2. (C) Configuration 3

Figure 14. The locations and postures of the furniture are consistent in all cases, even where the input waves are different and despite the contact parameters being uniformly set to the same values. In particular, a slight shift in the upper, separated cabinets in Figure 14a, the appearance of the tall cabinet leaning against the desk in Figure 14b, and the locations of furniture in Figure 14c and d are all in good agreement.

Moreover, to compare the motion of the furniture in detail during the rocking motion, the displacements measured by the motion capture system were investigated. The locations of luminous markers to evaluate displacements were set as shown in Figure 15. It was expected that the upper cabinet of the separated cabinets would exhibit complex motion behavior, and that the desk at the center of the shake-table would display a rocking motion while the office chair with casters slid across the floor.

First, the displacements in the *X*-axis direction of the upper, separated cabinets in configuration 3 under 50% and 100% 1-D JMA-Kobe waves, 100% 3-D JMA-Kobe wave, and 100% 3-D KiK-net Haga wave are shown in Figure 16. The numerical and experimental results agree well in the case of Figure 16a, where the magnitude of the input wave was

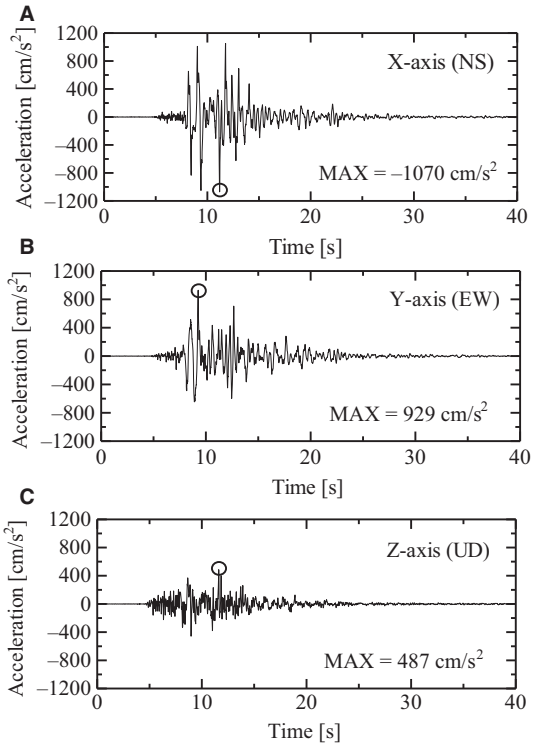

Figure 8. JMA-Kobe seismic wave. (A) *X*-axis (NS). (B) *Y*-axis (EW). (C) *Z*-axis (UD)

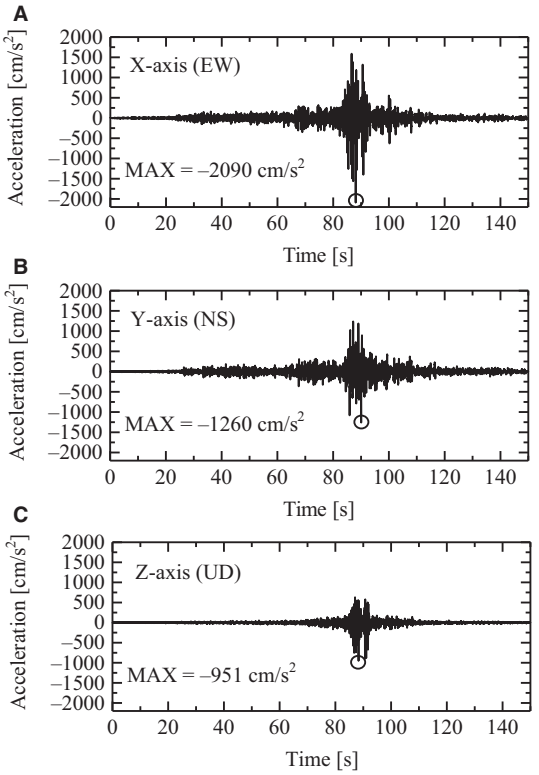

Figure 9. KiK-net Haga seismic wave. (A) *X*-axis (EW). (B) *Y*-axis (NS). (C) *Z*-axis (UD)

comparatively weak, especially in the timing of the rebound from the walls and the maximum displacement values. Furthermore, the timing of the fall of the upper cabinet after 3-5 s is

Table 3. Excitation program

Input wave	Excited direction	Input level
JMA-Kobe seismic wave	1-D (NS)	50%
		100%
	3-D	50%
		100%
KiK-net Haga seismic wave	1-D (EW)	50%
		100%
	3-D	50%
		100%

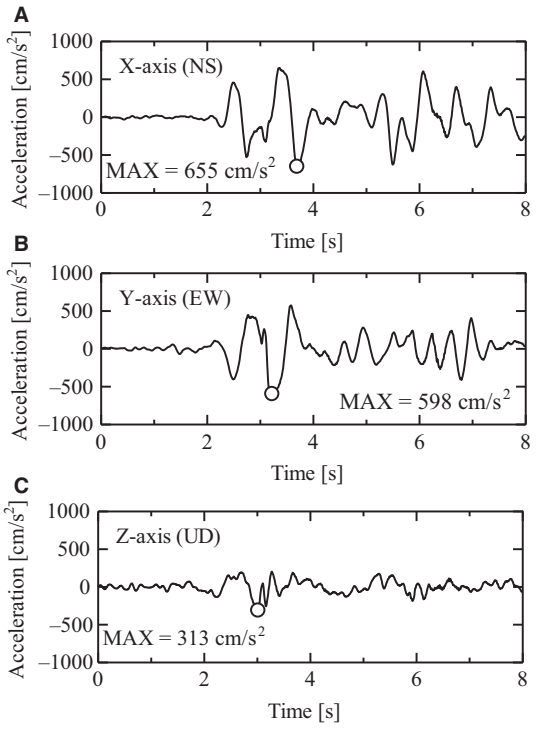

Figure 10. Acceleration observed on the shake-table when 100% JMA-Kobe wave was applied (only the part shown used for analysis). (A) *X*-axis (NS). (B) *Y*-axis (EW). (C) *Z*-axis (UD)

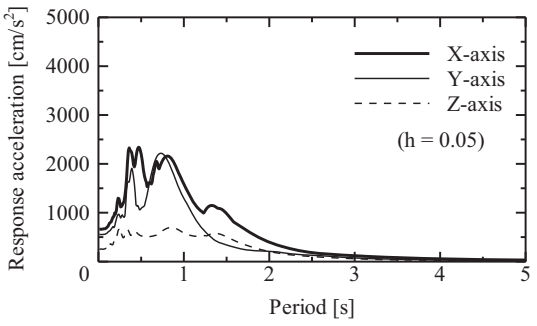

Figure 11. Acceleration response spectrum when 100% JMA-Kobe wave was applied (only the part shown used for analysis)

in good agreement, as shown in Figure 16b-d. The motions of the separated cabinets were simulated very well because they were placed against the wall and the motions were relatively restricted. The reasons why some experimental data are lost after the halfway point are that some markers came off during the excitation and some became hidden behind other furniture.

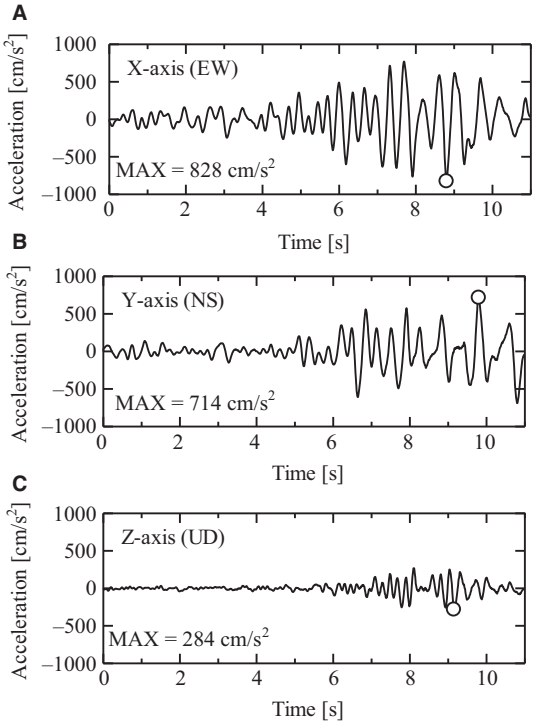

Figure 12. Acceleration observed on the shake-table when 100% KiK-net Haga wave was applied (only the part shown used for analysis). (A) *X*-axis (EW). (B) *Y*-axis (NS). (C) *Z*-axis (UD)

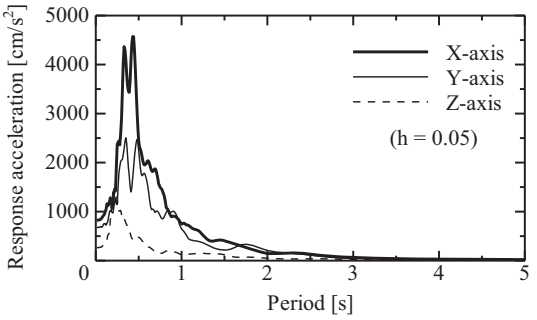

Figure 13. Acceleration response spectrum when 100% KiK-net Haga wave was applied (only the part shown used for analysis)

A comparison of the displacements in the *X*-axis direction at the evaluation point on the desk is shown in Figure 17. In the case of Figure 17a, with a comparatively weak magnitude of the input wave, the desk moves about 10 cm in the analysis, although almost no motion occurs in the experiment. Other results shown in Figure 17b-d indicate 10-30 cm differences, although the amplitudes of the displacements match well. This could be caused by initial errors in the fixed contact parameters, or the transition of the dynamic friction coefficients from moment to moment due to the change of contact face between the desk and the floor when the desk makes a rocking motion; the desk actually moved vertically upward by about 10 cm. Interference from other furniture, such as the tall cabinet falling on the desk after approximately 4 s in Figure 17c, is another possibility.

Finally, a comparison of the displacements in the *X*-axis direction at the evaluation point on the office chair with casters is shown in Figure 18. The coefficients of friction should vary depending on the direction of the casters. Therefore, the caster wheels were all aligned to the *X*-axis direction before each excitation. In the numerical analyses, however, the coefficients of dynamic friction were fixed to the value given in Table 4. The displacements in Figure 18a (comparatively weak magnitude of the input wave) agree well, because the uncertainty was reduced by aligning the caster wheels to the *X*-axis direction in the initial state. However, differences appear after approximately 4 s in the cases of Figure 18b-d. The direction dependency of the caster wheels is one reason, but there is again a strong possibility of interference from other furniture.

Furthermore, the shear forces that occurred in the element near the evaluation point on the desk were confirmed for the 100% 3-D JMA-Kobe wave. Figure 19 shows the shear forces in the vertical downward direction and depth direction on the top board. The shear forces reached a peak value after approximately 6.4 s, when the tall cabinet fell and collided with the element. The maximum values were −174 N vertically downward and 25 N in the depth direction on the top board, respectively. The ability to determine the sectional forces occurring in the furniture is one of the main advantages of using FEM.

6. Conclusions

In this study, a sophisticated penalty method for simulating complex contact phenomena between objects was implemented, and a finite element code to simulate motion behavior and the transition of sectional forces was developed. Various shake-table tests were conducted by arranging a set of furniture and applying two types of seismic waves at two input levels in 1-D and 3-D. Valuable information for selecting the numerical parameters was obtained from the results with less

Table 4. Contact parameters used in the analyses

Types of furniture	Penalty coefficient α (kgf)	Coefficient related to damping D_c (kgf)	Coefficient of dynamic friction μ			
			Contact on floor		Contact to walls	Between furniture
			Longer edge direction	Shorter edge direction		
Tall cabinet	43.6	52.3[a]	0.278[b]	0.208[b]	0.278	0.169
Upper, separated cabinet	21.3	25.6[a]	0.169[b]	0.169[b]	0.169	
Lower, separated cabinet	28.8	34.6[a]	0.230[b]	0.270[b]	0.270	
Side table	8.0	9.6[a]	0.094[b,c]	0.144[b]	0.144	
Desk	30.5	36.6[a]	0.377[b]	0.354[b]	0.377	
Office chair	6.2	7.4[a]	0.065[b]	0.038[b,c]	0.065	

[a]Penalty coefficient ×1.2. [b]Coefficient of static friction ×0.8. [c]Caster wheels of side table and chair were aligned to *X*-axis direction.

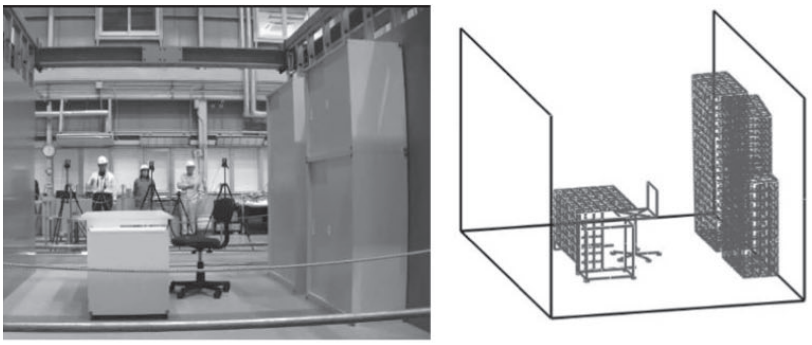

A 50 % JMA-Kobe wave, 1-D excitation

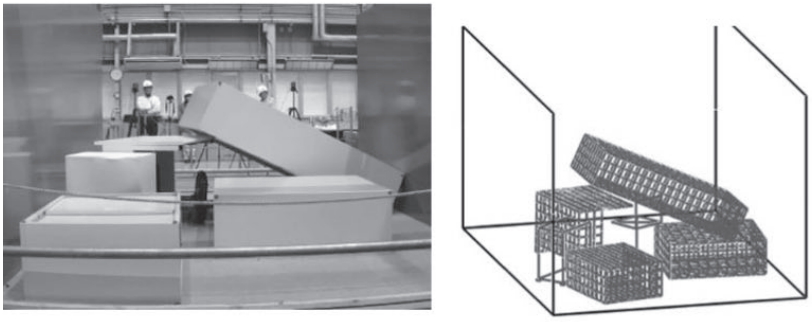

B 100 % JMA-Kobe wave, 1-D excitation

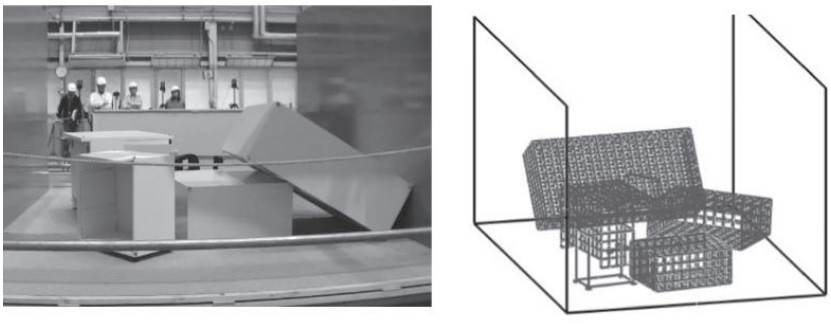

C 100 % JMA-Kobe wave, 3-D excitation

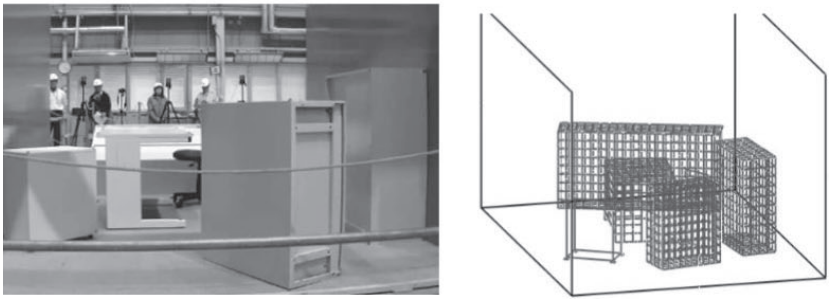

D 100 % KiK-net Haga wave, 3-D excitation

Figure 14. Appearances of furniture at the final states of experiments and analyses (configuration 3). (A) 50% JMA-Kobe wave, 1-D excitation. (B) 100% JMA-Kobe wave, 1-D excitation. (C) 100% JMA-Kobe wave, 3-D excitation. (D) 100% KiK-net Haga wave, 3-D excitation

interference between furniture, and the configuration guidelines for contact parameters were determined as follows:

1. Penalty coefficient: weight of furniture
2. Penalty index: 1
3. Damping coefficient: 120% of penalty coefficient
4. Dynamic friction coefficient: 80% of static friction coefficient

Using a motion capture system, the displacements obtained by the experiment and the analysis were compared to validate

Figure 15. Locations of evaluation points of displacements

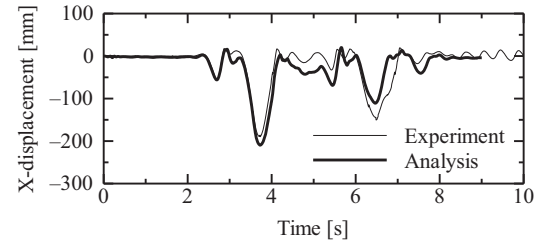

A 50 % JMA-Kobe wave, 1-D excitation

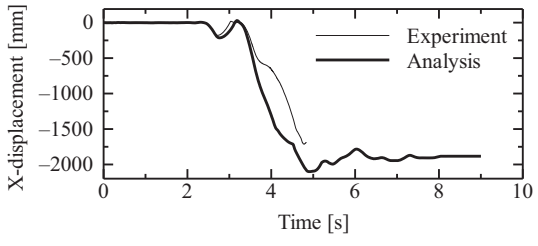

B 100 % JMA-Kobe wave, 1-D excitation

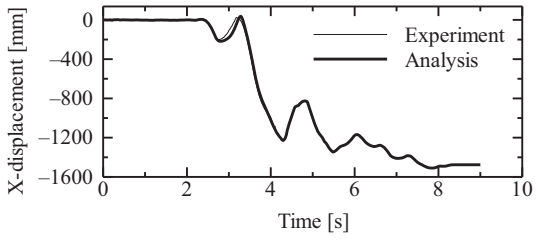

C 100 % JMA-Kobe wave, 3-D excitation

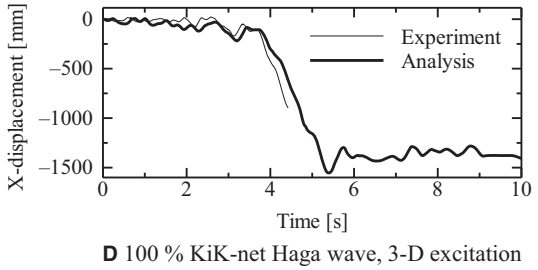

D 100 % KiK-net Haga wave, 3-D excitation

Figure 16. Comparison of displacements (upper, separated cabinets, configuration 3). (A) 50% JMA-Kobe wave, 1-D excitation. (B) 100% JMA-Kobe wave, 1-D excitation. (C) 100% JMA-Kobe wave, 3-D excitation. (D) 100% KiK-net Haga wave, 3-D excitation

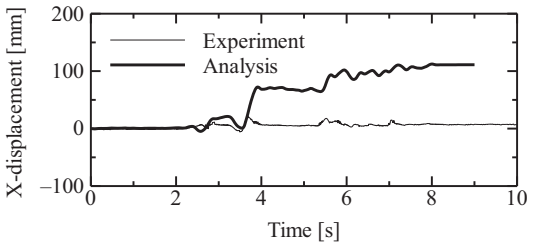

A 50 % JMA-Kobe wave,1-D excitation

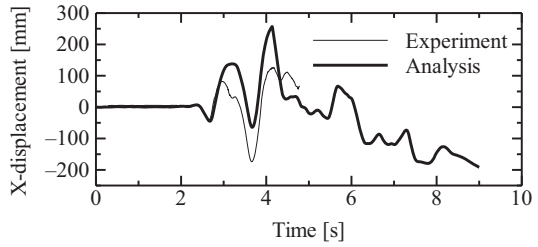

B 100 % JMA-Kobe wave, 1-D excitation

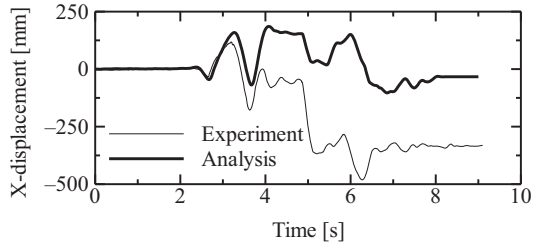

C 100 % JMA-Kobe wave, 3-D excitation

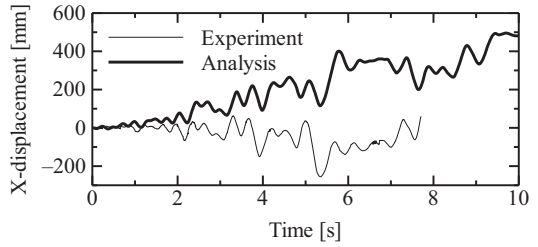

D 100 % KiK-net Haga wave, 3-D excitation

Figure 17. Comparison of displacements (desk, configuration 3). (A) 50% JMA-Kobe wave, 1-D excitation. (B) 100% JMA-Kobe wave, 1-D excitation. (C) 100% JMA-Kobe wave, 3-D excitation. (D) 100% KiK-net Haga wave, 3-D excitation

the numerical code and verify the above guidelines. It was confirmed that, although some differences in displacements were caused by interference between furniture, the numerical code can successfully simulate the motion behavior of furniture to a practical level, such as falling patterns and amplitudes of displacements, even though the input wave conditions were varied as follows:

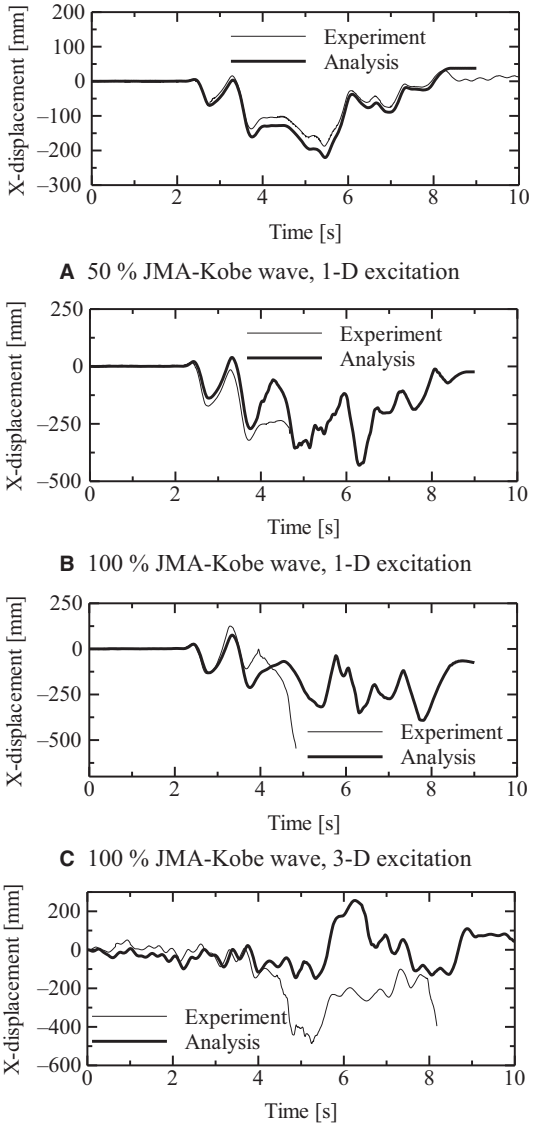

Figure 18. Comparison of displacements (office chair, configuration 3). (A) 50% JMA-Kobe wave, 1-D excitation. (B) 100% JMA-Kobe wave, 1-D excitation. (C) 100% JMA-Kobe wave, 3-D excitation. (D) 100% KiK-net Haga wave, 3-D excitation

i. Different input levels (50% and 100%)
ii. Different dimensions of excitation (1-D and 3-D)
iii. Different seismic waves (JMA-Kobe and KiK-net Haga waves)

However, there are several limitations when modeling furniture using the developed code. First, the code only uses beam elements and the center of gravity of the furniture must be adjusted by changing the densities of the beam elements. The strength of thin plates on the surface of furniture, for example, should be replaced by the stiffness of beam elements.

The computation time of the developed numerical code is long compared to that of DEM. However, the code successfully obtained information on the shear forces that occur in the furniture. Although further validations of such sectional forces should be carried out using experimental data, this should

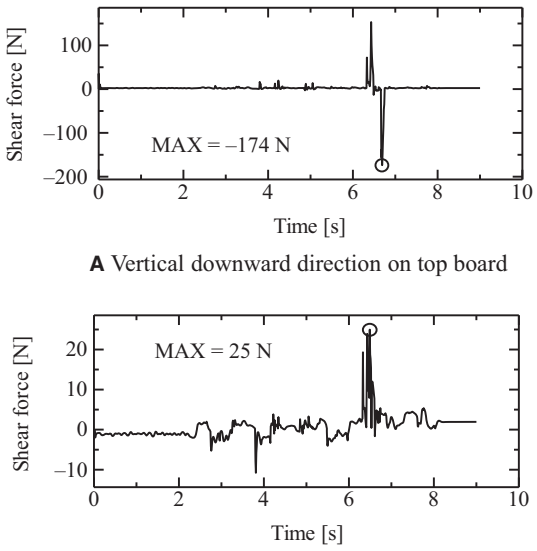

Figure 19. Shear forces occurred at evaluation point on the desk (100% JMA-Kobe wave, 3-D excitation, configuration 3). (A) Vertical downward direction on top board. (B) Depth direction on top board

provide useful information for discussing the safety of furniture that might fall on human bodies. Some modeling and analyses of furniture with quake-proof equipment, and verification of the effects, are planned in the future.

Acknowledgments

This work was carried out as one of the projects of the Facility Working Group of the E-Simulator Research & Development Committee, E-Defense, NIED. The authors would like to acknowledge the contribution of Dr. Masaaki Saruta of the Institute of Technology, Shimizu Corporation, for the shake-table tests. The contribution of Mr. Jiajie Gu of Mitsubishi Nichiyu Forklift Co., Ltd. (former graduate student of Univ. of Tsukuba) for the motion behavior analyses of furniture is also acknowledged.

Disclosure

The authors have no conflict of interest to declare.

References

1 Architectural Institute of Japan. *Report on Investigation of Indoor Damages during the Great Hanshin-Awaji Earthquake*. Tokyo, Japan: Architectural Institute of Japan; 1996.
2 Enokida R, Nagae T, Kajiwara K, Ji X, Nakashima M. Development of shaking table test techniques to realize large responses and evaluation of safety of a high-rise building. *J Struct Constr Eng (Trans AIJ)*. 2009;**74**:467-476 (in Japanese).
3 Cundall PA. A computer model for simulating progressive, large-scale movement in blocky rock system. Proceedings of the International Symposium on Rock Mechanics, II-8, pp. 129-136, 1971.
4 Kaneko M, Hayashi Y. Proposal of a curve to describe overturning ratios of rigid bodies. *J Struct Constr Eng (Trans AIJ)*, No. 536, pp. 55-62, 2000 (in Japanese).
5 Masatsuki T, Midorikawa S, Ohori M, Miura H. Simulation for seismic behavior of office furniture in a high-rise building. *J Struct Constr Eng (Trans AIJ)*, No. 620, pp. 43-49, 2007 (in Japanese).
6 Fujita H, Takahashi T, Nakamura Y, Yamashita Y, Isobe D. Estimation using distinct element method on test result of E-defense examination concerning an indoor situation on strong motion for important facilities. Summaries of Technical Papers of Annual Meeting Architectural Institute of Japan, B-2, pp. 671-672, 2013.

7 Yamashita T, Hori M, Kajiwara K. Petascale computation for earthquake engineering. *Computing in Science and Engineering*. 2011;**13**:44-49.
8 Isobe D, Lynn KM. Structural collapse analysis of steel framed structure due to aircraft collision. *J Struct Constr Eng (Trans AIJ)*. 2004;**69**:39-46 (in Japanese).
9 Yagawa G, Hirayama H, Ando Y. Analysis of two-dimensional bodies and beams in contact using penalty function method. *Trans Jpn Soc Mech Eng Ser A*. 1980;**46**:1220-1229 (in Japanese).
10 Toi Y, Isobe D. Adaptively shifted integration technique for finite element collapse analysis of framed structures. *Int J Numer Methods Eng*. 1993;**36**:2323-2339.

How to cite this article: Isobe D, Yamashita T, Tagawa H, Kaneko M, Takahashi T, Motoyui S. Motion analysis of furniture under seismic excitation using the finite element method. *Jpn Archit Rev*. 2018;1:44–55. https://doi.org/10.1002/2475-8876.1015